UC Berkeley
UC Berkeley Previously Published Works

Title
High-SPL and Low-Driving-Voltage pMUTs by Sputtered Potassium Sodium Niobate

Permalink
https://escholarship.org/uc/item/6b89s0g2

Authors
Xia, Fan
Peng, Yande
Pala, Sedat
et al.

Publication Date
2023-01-19

DOI
10.1109/mems49605.2023.10052391

Copyright Information
This work is made available under the terms of a Creative Commons Attribution License, available at https://creativecommons.org/licenses/by/4.0/

Peer reviewed

eScholarship.org Powered by the California Digital Library
University of California

HIGH-SPL AND LOW-DRIVING-VOLTAGE PMUTS BY SPUTTERED POTASSIUM SODIUM NIOBATE

Fan Xia[1,2], Yande Peng[1,2], Sedat Pala[1,2], Ryuichi Arakawa[1,3], Wei Yue[1,2], Pei-Chi Tsao[2], Chun-Ming Chen[2], Hanxiao Liu[1,2], Megan Teng[2], Jong Ha Park[1,2], and Liwei Lin[1,2]

[1]Berkeley Sensor and Actuator Center, Berkeley, CA, USA

[2]Department of Mechanical Engineering, University of California, Berkeley, CA, USA and

[3]NGK Spark Plug Co., JAPAN

2023 IEEE 36th International Conference on Micro Electro Mechanical Systems (MEMS) | 978-1-6654-9308-6/23/$31.00 ©2023 IEEE | DOI: 10.1109/MEMS49605.2023.10052391

ABSTRACT

This work presents an air-coupled piezoelectric micromachined ultrasonic transducer (pMUT) with high transmitting acoustic pressure by using sputtered potassium sodium niobate (K,Na)NbO_3 (KNN) thin film with a high piezoelectric coefficient (e_{31} ~ 8-10 C/m^2) and low dielectric constant (ϵ_r ~ 260-300) for the first time. The fabricated KNN pMUT with a resonant frequency at 104.5 kHz has been tested to exhibit unprecedented results: (1) high sound pressure level (SPL) of 109 dB/V at a distance of 10 cm, which is 8 times higher than that of AlN-based pMUTs at a similar frequency; (2) low-voltage operation of only 4 volts peak-to-peak amplitude (V_{p-p}); and (3) good receiving sensitivity. As such, this work presents a new class of high-SPL and low-driving-voltage pMUTs for potential applications in various fields, including consumer electronics, such as but not limited to haptic feedback, loudspeaker, and AR/VR systems.

KEYWORDS

Ultrasound, pMUT, acoustic pressure, low driving voltage, piezoelectric, KNN.

INTRODUCTION

Ultrasonic transducers are widely used in robotics and automotives for object detection. Compared with the bulk ultrasonic transducers, the small-footprint piezoelectric micromachined ultrasonic transducers (pMUTs) have low power consumption and wide bandwidth for applications in consumer electronics and Internet of Things (IoT), such as range-finding [1], gesture recognition [2], fingerprint sensing [3], and 3D imaging [4]. However, relatively low output pressure remains a significant challenge for AlN-based pMUTs, which limits the signal transmissions in various applications. For instance, state-of-the-art AlN-based rangefinder can only reach a travel distance of 4 m with an array design [5]. For other applications where large acoustic pressure output is critical, such as mid-air haptic feedback [6], this becomes an engineering challenge.

It is well-known that the transmitting performance of pMUTs is mainly determined by the device structure and piezoelectric material property. Continuous efforts have been made in optimizing the device structures, such as to modify the boundary condition [7], construct the bimorph architecture [8] and adjust the mode shape [9]. Even so, the output pressure of pMUT is still limited by the intrinsically low piezoelectric coefficient of the material such as AlN with the e_{31} around 1 C/m^2. There are also reports on increasing the piezoelectric coefficient of materials by tuning material compositions, for example, the scandium-doped AlN [10]. Other materials, like lead zirconate titanate (PZT)-based pMUTs [11,12] have relatively higher output pressure, but their low receiving sensitivity and the lead-contents are key drawbacks. Thus, there's a strong need for better piezoelectric materials of batch fabrication process to further boost the performance of pMUTs.

Here, we report an air-coupled pMUT based on sputtered, lead-free KNN thin film with high piezoelectric coefficient (e_{31} ~ 8-10 C/m^2) and low dielectric constant (ϵ_r ~ 260-300) for the first time. The excellent transmitting sensitivity (8 times higher than that of AlN-based pMUTs) and good receiving performance under a low-voltage excitation are demonstrated.

DESIGN AND FABRICATION

Principle of Design

Figure 1a shows the structure of KNN pMUTs with a circular unimorph diaphragm. The device consists of the 2-um sensor-type KNN thin film [13] as the active piezoelectric layer and a 5-um Si device layer as the elastic layer. The dual-electrode geometry has a circular-shape inner electrode (67% in radius [14]) and a ring-shape outer electrode. The differential drive can be applied, where the inner and outer electrode are excited with opposite polarity to enhance the vibration displacement and output pressure correspondingly. The simulated fundamental mode shape with clamped boundary condition is shown in **Figure 1b**.

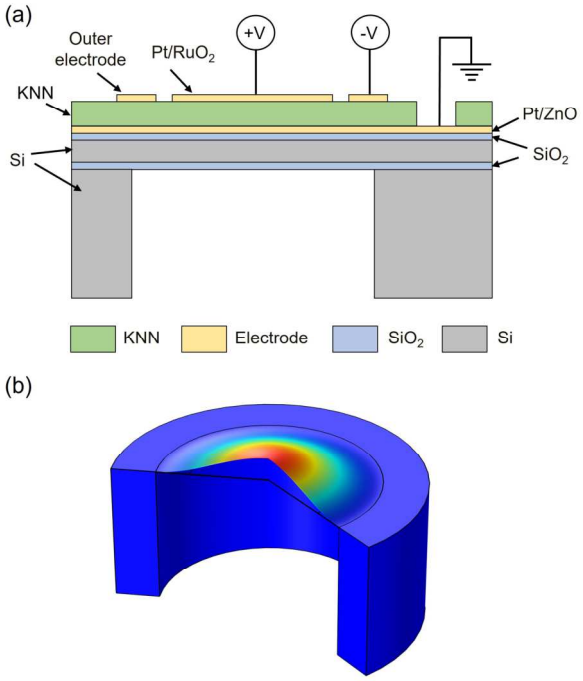

Figure 1: (a) The schematic cross-sectional view of a dual electrode, circular unimorph KNN pMUT; (b) simulated fundamental mode shape.

Authorized licensed use limited to: Univ of Calif Berkeley. Downloaded on August 02,2024 at 20:59:27 UTC from IEEE Xplore. Restrictions apply.

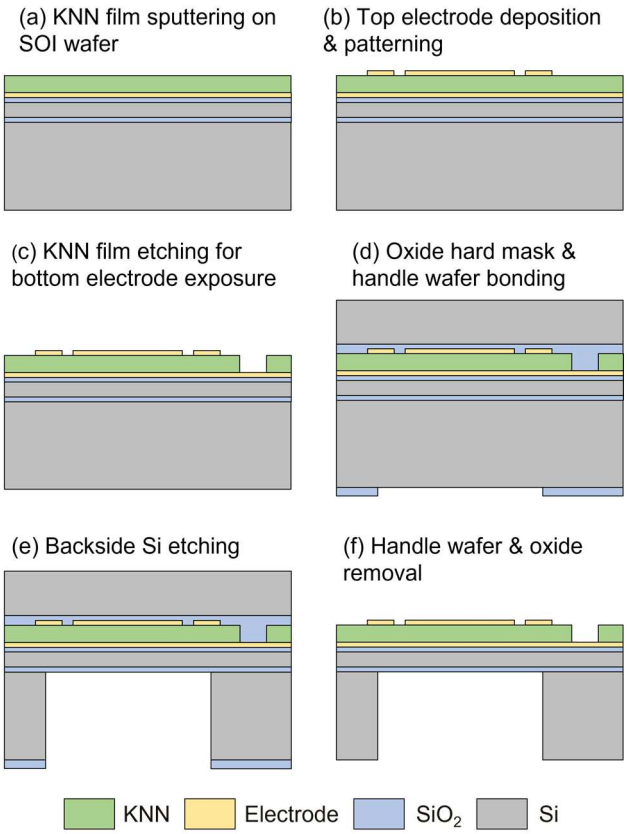

Figure 2: Fabrication process.

Fabrication process

The detailed fabrication process is shown in **Figure 2**. The process starts with the sputtering of 25 nm-thick ZnO adhesion layer and 200 nm-thick Pt bottom electrode on a 6-inch SOI wafer which consists of a 5 um-thick Si device layer, 1 um-thick buried silicon oxide (BOX) layer and 610 um-thick (100) Si handle substrate. Then 2 um-thick KNN thin film which serves as the active piezoelectric layer, is deposited via a radio frequency (RF) magnetron-sputtering process on top of the Pt/ZnO bottom electrode layer. After that, 10 nm-thick RuO_2 and 100 nm-thick Pt are sputtered and patterned as the inner circular and outer ring Pt/RuO_2 top electrode, where RuO_2 is used to promote the adhesion strength between Pt and KNN thin film [13]. Afterwards, the via openings to access the bottom electrode is realized by patterning the KNN film through a wet-etching process. Finally, backside silicon cavity is defined by a deep reactive-ion etching (DRIE) process where the BOX layer acts as the etching stop layer, and the device wafer is temporarily bonded to a handle wafer during the process.

RESULTS

Characterization

Figure 3-4 shows the characterization results of the fabricated KNN pMUTs. The crystal structure of the sputtered KNN film is characterized by using the X-ray diffraction to monitor the film quality, and the sharp peak in the (001) orientation confirms its perovskite structure with good crystallinity (**Figure 3**). The benign surface morphology is highlighted by the optical image of the pMUTs as well (**Figure 4a-4b**).

The cross-sectional scanning electron microscope (SEM) images, as shown in **Figure 4c-4d**, display the well-defined backside silicon cavity, the tightly stacked Pt/RuO_2/KNN/Pt/ZnO/SiO_2/Si multi-layered diaphragm structure, and further show the thickness of each layer (1.9 um-thick KNN and 5.2 um-thick Si device layer). The dense columnar structure of the KNN thin film validates the good crystal orientation which plays an important role in the piezoelectric performances.

Transmission performance

The transmission pressure of a single KNN pMUT with a radius of 500 um is measured utilizing a high-sensitivity microphone (Bruel & Kjar, Type 4138). The prototype KNN pMUT is driven by continuous differential sine-wave signals for the inner and outer electrodes. The receiving signal is collected by placing the microphone 1 cm above the pMUT and the sound pressure level (SPL) is extracted through the corresponding sensitivity. As shown in **Figure 5a**, a maximum transmission pressure of 135.7 dB SPL (121.73 Pa) is achieved at 104.5 kHz with the 4 V_{p-p} excitation, and the non-linear hardening phenomena can be observed near the peak [15].

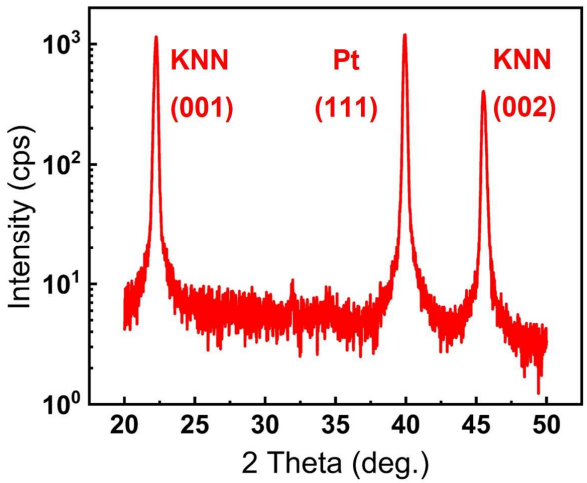

Figure 3: XRD of sputtered KNN thin film with (001) crystal orientation.

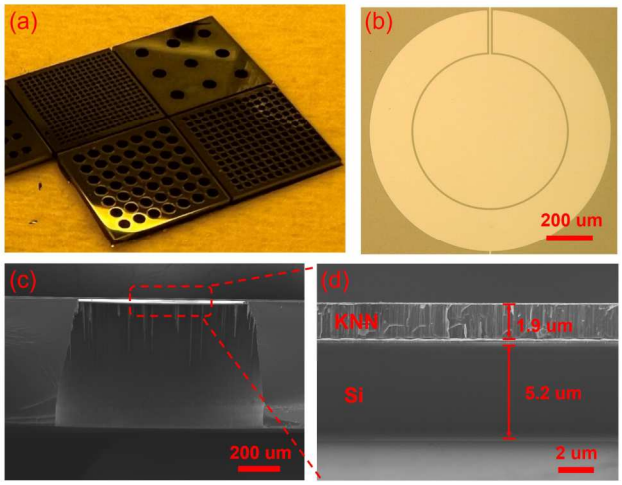

Figure 4: Characterization results. (a) Backside of KNN pMUTs with different sizes; (b) a microscope top image of prototype KNN pMUT; (c-d) cross-sectional SEM images.

Authorized licensed use limited to: Univ of Calif Berkeley. Downloaded on August 02,2024 at 20:59:27 UTC from IEEE Xplore. Restrictions apply.

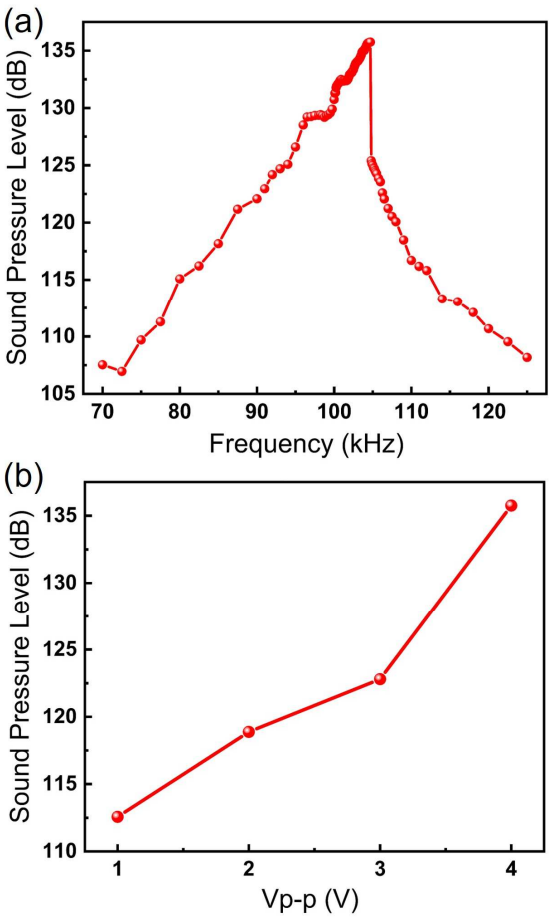

Figure 5: Transmission performance of single KNN pMUT. Sound pressure level (SPL) @ 1 cm axial distance versus (a) frequency, and (b) excitation voltage (V_{p-p}).

The influences of excitation voltage and axial distance on the transmission pressure are further evaluated at 104.5 kHz. As shown in **Figure 5b**, the SPL at 1 cm axial distance increases from 112.6 dB (8.5 Pa) to 135.8 dB (122.71 Pa) as V_{p-p} increases from 1 V to 4 V. **Figure 6** shows the relationship between the SPL and axial distance, where the SPL under a 4 V_{p-p} input gradually decreases from 150.5 dB (666.85 Pa) @ 0.1cm to 115.1 dB (11.3 Pa) @ 10cm, and 102.6 dB (2.71 Pa) @ 30 cm. Thus, the transmission sensitivity of the single KNN pMUT reaches 129.3 dB/V SPL (58.27 Pa/V) @ 1 cm, 109 dB/V SPL (5.66 Pa/V) @10 cm, and 96.6 dB/V SPL (1.36 Pa/V) @ 30 cm axial distance.

Finally, a summary of the transmission performance comparison with other devices in the state-of-the-art literature is shown in Table 1. The KNN pMUT stands out with its transmitting sensitivity 8~10 times higher than those of AlN pMUTs, highlighting its extraordinary advantage of high SPL under a low driving voltage.

Receiving performance

The receiving performance is evaluated by using two identical pMUTs (500 um in radius) as the transmitter (T_x) and receiver (R_x) respectively. The pMUT transmitter is excited via 7-cycle sine-wave pulse signal (104.5 kHz, 4 V_{p-p}) with the differential drive scheme. For the receiving pMUT, only the inner region is utilized. Furthermore, a charge amplifier is applied, and the amplified receiving signals with respect to distances are measured. **Figure 7a** exhibits the excitation and receiving signal with a travel distance of 2 m. The receiving signal peak-value has a Time-of-Flight (ToF) of 6.13 ms which matches well with the real distance measured by the laser distance meter. The relationship between the receiving signal magnitude and travel distance is displayed in **Figure 7b**, and the signal can be clearly identified with the travel distance up to 6.1 m (3 m for the round trip), demonstrating good receiving performance.

CONCLUSION

This work has demonstrated the first sputtered KNN-based pMUTs. The KNN film exhibits good crystal quality in (001) orientation, which contributes to the high piezoelectric coefficient. The fabricated KNN pMUT with a resonant frequency of 104.5 kHz is used to evaluate the transmission and receiving performance. Specifically, a high SPL of 135.8 dB can be obtained from the single pMUT with axial distance of 1 cm under a low driven voltage of 4 V_{p-p}, and it remains larger than 100 dB with distance up to 40 cm. The corresponding transmission sensitivity turns out to be 8 times larger than that of the state-of-the-art AlN-based pMUTs. The good sensitivity is also demonstrated by the clear receiving signal which travels up to 6.1 m. As such, this work sheds light on high-SPL and low-driving-voltage pMUTs for potential applications, like haptic feedback, loudspeaker, and AR/VR systems.

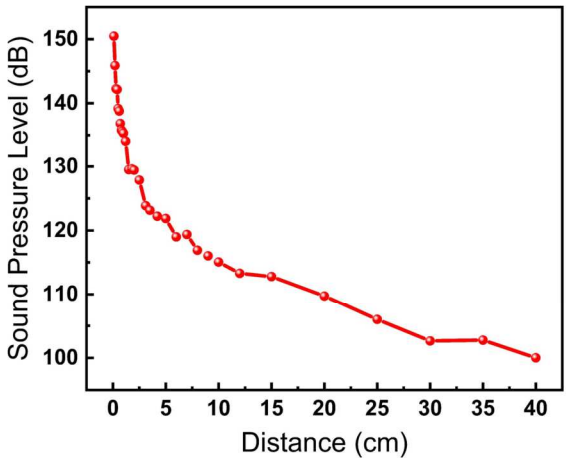

Figure 6: SPL @ resonance under the continuous sine-wave excitation (4 V_{p-p}) versus the axial distance.

Table 1: Transmission sensitivity comparison with other devices in the state-of-the-art literature.

Material	Frequency	V_{p-p}	SPL (dB/V)	Ref.
AlN	101k	20	90@10 cm	[4]
36% Sc doped AlN	60k	/	71.6@30 cm	[10]
Single-crystal PZT	46k	10	93@14.4 cm 86.3@33 cm	[11]
PZT	100k	6	93.5@3.5 cm	[12]
PMN-PZT	151k	3	94.6@6 cm; 88.6@13 cm	[16]
KNN	**104.5k**	**4**	**109@10 cm; 96.6@30 cm**	**This work**

Authorized licensed use limited to: Univ of Calif Berkeley. Downloaded on August 02,2024 at 20:59:27 UTC from IEEE Xplore. Restrictions apply.

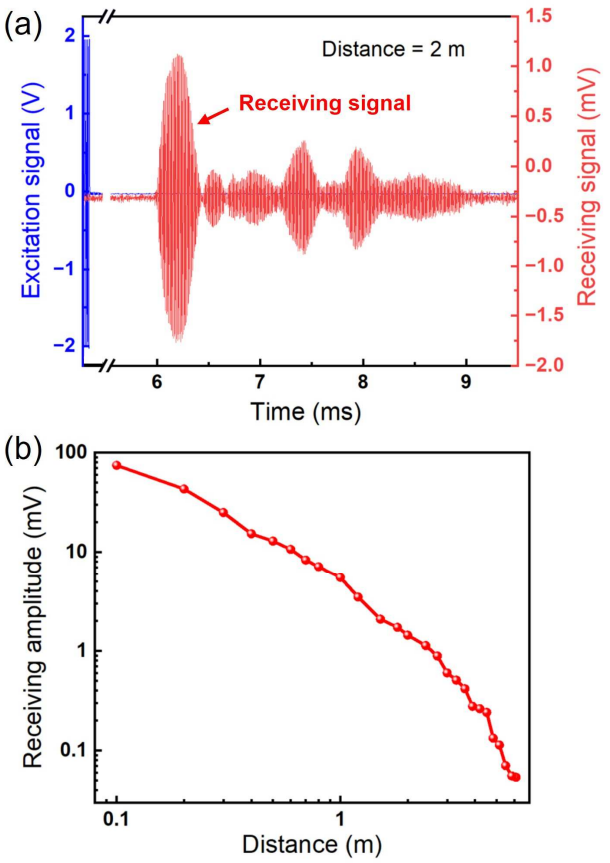

Figure 7: Receiving performance. (a) Amplified receiving signal with a travelling distance of 2 m; (b) the receiving signal magnitude vs the travel distance.

ACKNOWLEDGEMENTS

This work was supported in part by BSAC (Berkeley Sensor and Actuator Center) and the NSF grant ECCS-2128311. The authors thank SCIOCS Co. Ltd. for KNN film deposition/etching processes, UC Berkeley Marvell Nanofabrication Lab for the rest of the fabrication process.

REFERENCES

[1] R. J. Przybyla, S. E. Shelton, A. Guedes, I. I. Izyumin, M. H. Kline, D. A. Horsley, and B. E. Boser. "In-air rangefinding with an aln piezoelectric micromachined ultrasound transducer", *IEEE Sensors Journal* 11, no. 11 (2011): 2690-2697.

[2] R. J. Przybyla, H. Tang, S. E. Shelton, D. A. Horsley, and B. E. Boser. "12.1 3D ultrasonic gesture recognition", in *2014 IEEE International Solid-State Circuits Conference Digest of Technical Papers (ISSCC)*, pp. 210-211. IEEE, 2014.

[3] X. Jiang, H. Tang, Y. Lu, E. J. Ng, J. M. Tsai, B. E. Boser, and D. A. Horsley. "Ultrasonic fingerprint sensor with transmit beamforming based on a PMUT array bonded to CMOS circuitry", *IEEE Trans. Ultrason. Ferroelectr. Freq. Control*, 64, no. 9 (2017): 1401-1408.

[4] Z. Shao, Y. Peng, S. Pala, Y. Liang, and L. Lin. "3D ultrasonic object detections with> 1 meter range", in *2021 IEEE 34th International Conference on Micro Electro Mechanical Systems (MEMS)*, pp. 386-389. IEEE, 2021.

[5] Z. Shao, S. Pala, Y. Peng, and L. Lin. "Bimorph Pinned Piezoelectric Micromachined Ultrasonic Transducers for Space Imaging Applications", *J. Microelectromech. Syst.*, 30, no. 4 (2021): 650-658.

[6] S. Pala, Z. Shao, Y. Peng, and L. Lin. "Ultrasond-induced haptic sensations via PMUTS", in *2021 IEEE 34th International Conference on Micro Electro Mechanical Systems (MEMS)*, pp. 911-914. IEEE, 2021.

[7] Y. Liang, B. Eovino, and L. Lin. "Piezoelectric micromachined ultrasonic transducers with pinned boundary structure", *J. Microelectromech. Syst.*, 29, no. 4 (2020): 585-591.

[8] S. Akhbari, F. Sammoura, B. Eovino, C. Yang, and L. Lin. "Bimorph piezoelectric micromachined ultrasonic transducers", *J. Microelectromech. Syst.*, no. 2 (2016): 326-336.

[9] T. Wang, R. Sawada, and C. Lee. "A piezoelectric micromachined ultrasonic transducer using piston-like membrane motion", *IEEE Electron Device Letters*, 36, no. 9 (2015): 957-959.

[10] Y. Kusano, I. Ishii, T. Kamiya, A. Teshigahara, G. Luo, and D. A. Horsley. "High-SPL air-coupled piezoelectric micromachined ultrasonic transducers based on 36% ScAlN thin-film", *IEEE Trans. Ultrason. Ferroelectr. Freq. Control*, 66, no. 9 (2019): 1488-1496.

[11] G. Luo, Y. Kusano, M. N. Roberto, and D. A. Horsley. "High-pressure output 40 kHz air-coupled piezoelectric micromachined ultrasonic transducers", in *2019 IEEE 32nd International Conference on Micro Electro Mechanical Systems (MEMS)*, pp. 787-790. IEEE, 2019.

[12] G. Massimino, L. D'Alessandro, F. Procopio, R. Ardito, M. Ferrera, and A. Corigliano. "Air-coupled PMUT at 100 kHz with PZT active layer and residual stresses: Multiphysics model and experimental validation", in *2017 18th International Conference on Thermal, Mechanical and Multi-Physics Simulation and Experiments in Microelectronics and Microsystems (EuroSimE)*, pp. 1-4. IEEE, 2017.

[13] K. Shibata, K. Watanabe, T. Kuroda, and T. Osada. "KNN lead-free piezoelectric films grown by sputtering", *Appl. Phys. Lett.*, 121, no. 9 (2022): 092901.

[14] S. Pala, and L. Lin. "An Improved Lumped Element Model for Circular-shape pMUTs", *IEEE Open Journal of Ultrasonics, Ferroelectrics, and Frequency Control (2022)*.

[15] G. Massimino, B. Lazarova, F. Quaglia, and A. Corigliano. "Air-coupled PMUTs array with residual stresses: experimental tests in the linear and non-linear dynamic regime", *Int. J. Smart Nano Mater.*, 11, no. 4 (2020): 387-399.

[16] Z. Zhou, S. Yoshida, and S. Tanaka. "Epitaxial PMnN-PZT/Si MEMS ultrasonic rangefinder with 2 m range at 1 V drive", *Sens. Actuator A Phys.*, 266 (2017): 352-360.

CONTACT

*F. Xia, tel: +1-341-766-8361; fxia21@berkeley.edu

Authorized licensed use limited to: Univ of Calif Berkeley. Downloaded on August 02,2024 at 20:59:27 UTC from IEEE Xplore. Restrictions apply.